Journal of Scientific and Human Dimensions
مجلة الأبعاد العلمية والإنسانية
ISSN: 3106-1702
Volume 2, Issue 3, 2026 Pages: 140-148
Journal homepage: https://jshd.com.ly/index.php/jshd/en

Growth and Morphological Evolution of Porous Anodic Alumina via Two-Step Anodization in 0.3 M Oxalic Acid

Sanaa Masod Abdulqader [*1] , Najah Ibrahem Elharari [*2]
[1]Department of Physics Science, Faculty of Education/ Kikla, University of Gharyan, Libya
[2] Higher Institute of Medical Sciences and Technology / Abu salim, Libya

نمو وتطور البنية المسامية لألومينا مؤكسدة مسامية عبر الأكسدة الثنائية في حمض الأكساليك 0.3 مولار

سناء مسعود عبد القادر [*1]، نجاح ابراهيم الحراري [*2]
[1] قسم الفيزياء، كلية التربية - ككلة، جامعة غريان، غريان، ليبيا
[2] المعهد العالي للعلوم والتقنيات الطبية - أبو سليم، طرابلس، ليبيا

[*]Corresponding author: sanaamasod1985@gmail.com [1] , najahalhrari92@gmail.com [2]

Received: May 20, 2026	Accepted: June 25, 2026	Published: July 16, 2026

Abstract:
Porous anodic alumina (PAA) films were fabricated via a two-step anodization process in 0.3 M oxalic acid at 40 V. This study systematically investigates the effect of anodization duration on the morphology, pore diameter, surface roughness, and crystallographic texture of PAA using atomic force microscopy (AFM) and the Harris equation. Results demonstrate that increasing anodization time from 30 min to 4 h facilitates the formation of highly ordered hexagonal pore arrays. Specifically, the mean pore diameter increased from 45 ± 6 nm to 72 ± 4 nm, while surface roughness (Ra) decreased from 8.3 nm to 4.1 nm. Furthermore, the texture coefficient TC(111) increased from 2.1 to 9.0, indicating a strong preferred orientation. The sample anodized for 4 h exhibited optimal self-ordered morphology with straight pore channels and minimal structural defects. These findings confirm that anodization time is a critical parameter for achieving steady-state growth, providing quantitative guidelines for the fabrication of high-quality templates for nanophotonic and sensing applications.

Keywords: Porous Anodic Alumina; Two-Step Anodization; Oxalic Acid; Atomic Force Microscopy; Texture Coefficient; Harris Equation; Nanopores

الملخص
تم تحضير أغشية الألومينا المؤكسدة المسامية (PAA) باستخدام طريقة الأكسدة الثنائية في محلول حمض الأكساليك بتركيز 0.3 مولار عند جهد 40 فولت. هدفت هذه الدراسة إلى بحث تأثير زمن الأكسدة بشكل منهجي على البنية المجهرية، وقطر المسام، وخشونة السطح، والنسيج البلوري باستخدام مجهر القوة الذرية (AFM) ومعادلة "هاريس". أظهرت النتائج أن زيادة زمن الأكسدة من 30 دقيقة إلى 4 ساعات تؤدي إلى تكوين مصفوفة سداسية عالية الترتيب. حيث ارتفع متوسط قطر المسام من 45 ± 6 نانومتر إلى 72 ± 4 نانومتر، بينما انخفضت خشونة السطح (Ra) من 8.3 نانومتر إلى 4.1 نانومتر. علاوة على ذلك، ارتفع معامل النسيج TC(111) من 2.1 إلى 9.0، مما يشير إلى توجه بلوري مفضل قوي. أظهرت العينة التي خضعت للأكسدة لمدة 4 ساعات بنية نانوية مرتبة ذاتياً ومثالية، تميزت بقنوات مسامية مستقيمة وعيوب هيكلية دنيا. تؤكد هذه النتائج أن زمن الأكسدة يعد متغيراً حاسماً لتحقيق حالة النمو المستقر، مما يوفر معايير كمية لتصنيع قوالب عالية الجودة للتطبيقات النانوية والضوئية والحسية.

الكلمات المفتاحية: ألومينا مؤكسدة مسامية؛ أكسدة ثنائية؛ حمض الأكساليك؛ مجهر القوة الذرية؛ معامل النسيج؛ معادلة هاريس؛ مسام نانوية.

1. Introduction

Porous anodic alumina (PAA) has emerged as a cornerstone in the field of nanotechnology, garnering substantial attention due to its unique architectural properties, including highly ordered hexagonal nanopore arrays, precisely tunable pore diameters, high aspect ratios, and exceptional chemical and thermal stability (Masuda & Fukuda, 1995; Lee & Park, 2014). This self-organized material, synthesized through the electrochemical oxidation of aluminum substrates in acidic electrolytes, functions as a sophisticated template for the bottom-up fabrication of functional nanostructures, ranging from high-density nanowire arrays and photonic crystals to advanced filtration membranes and highly sensitive biomedical diagnostic platforms (Santos et al., 2017).

The morphological and structural integrity of PAA is intrinsically governed by a complex interplay of electrochemical parameters, primarily electrolyte composition, applied potential, operating temperature, and anodization duration (Sulka, 2008). Within the established "mild anodization" regime, typically utilizing oxalic acid at 40 V, the system exhibits a predictable interpore distance of approximately 100 nm, which adheres to the widely recognized proportionality constant of 2.5 nm/V (Jessensky et al., 1998). To overcome the structural limitations inherent in single-step processes, the two-step anodization technique has become the standard for achieving long-range hexagonal ordering. In this methodology, the initial anodization phase generates a disordered oxide layer that, upon selective chemical dissolution, leaves a periodic concave nanostructure on the aluminum surface; this pre-patterned landscape effectively acts as a geometric guide, facilitating the growth of highly ordered, vertical pore channels during the subsequent second anodization phase (Masuda et al., 2001).

Despite the foundational understanding of how voltage and electrolyte concentration influence PAA architecture, the kinetic evolution of morphology and the development of crystallographic texture under sustained mild anodization conditions remain areas requiring further rigorous investigation. It is hypothesized that prolonged anodization periods foster an enhanced degree of structural self-ordering by permitting the system to approach a dynamic steady-state equilibrium, where the rate of oxide formation at the metal/oxide interface is balanced by the field-assisted chemical dissolution at the oxide/electrolyte interface (Thompson, 1997). Furthermore, the refinement of this process is crucial for optimizing the mechanical and optical performance of the resulting PAA layers. In this context, the present study aims to provide a comprehensive, quantitative analysis of the time-dependent morphological evolution and texture development of PAA. By applying the Harris equation to interpret crystallographic orientation, this research systematically correlates anodization duration with pore uniformity, surface roughness, and textural characteristics, thereby establishing definitive optimization protocols for the fabrication of high-fidelity nanostructures.

2. Experimental Methods

2.1. Substrate Preparation

High-purity aluminum foil (99.99% purity, 0.25 mm thickness) was utilized as the starting material to minimize the influence of impurities on the anodization kinetics. The foil was precisely sectioned into 2 × 2 cm^2 substrates. To remove surface contaminants and organic residues, the samples underwent a rigorous degreasing process in an ultrasonic acetone bath for 10 min, followed by thorough rinsing with deionized water. Subsequently, to ensure an atomically smooth surface suitable for the nucleation of highly ordered nanopores, the samples were electropolished in a chilled mixture of perchloric acid ($HClO_4$) and ethanol (C_2H_5OH) in a 1:4 (v/v) ratio. This process was maintained at 20 V for 3 min at a controlled temperature of 5 °C, achieving a mirror-like finish with an average surface roughness (R_a) of less than 2 nm.

2.2. Two-Step Anodization Process

The fabrication of highly ordered porous anodic alumina (PAA) was carried out using a conventional two-electrode electrochemical cell, with the aluminum substrate serving as the anode and a platinum sheet as the cathode. The anodization electrolyte consisted of 0.3 M oxalic acid ($H_2C_2O_4$), maintained at a constant temperature of 5 ± 1 °C using a circulating chiller to prevent thermal runaway and localized burning of the oxide layer. A constant voltage of 40 V was applied throughout the process. The experimental design investigated three distinct anodization durations (30 min, 60 min, and 4 h) to evaluate their influence on morphological evolution. After the first anodization step, the resulting disordered oxide layer was selectively removed through chemical etching in a mixture of 6 wt% phosphoric acid (H_3PO_4) and 1.8 wt% chromic acid (H_2CrO_4) at 60 °C for 6 h. This etching procedure exposed a pre-patterned, hexagonal array of concave nanopits on the aluminum surface, which served as structural templates for guiding the highly ordered pore growth during the second anodization step, conducted under identical electrochemical conditions.

2.3. Structural and Morphological Characterization

The surface morphology and topographic features of the fabricated PAA films were characterized using Atomic Force Microscopy (AFM) in tapping mode. High-resolution images were captured over scan areas of 5 × 5 μm² and 2 × 2 μm². To ensure statistical significance, the morphological parameters were extracted from the AFM data using ImageJ software, with a sample size of at least 200 pores per specimen to derive mean pore diameters and interpore distances. Surface roughness (R_a) was systematically calculated from the 5 × 5 μm² scan areas utilizing Gwyddion analysis software. Furthermore, the porosity (P) of the PAA membranes was quantitatively determined by applying the geometric model for a hexagonal pore arrangement, defined by the formula:

$$P = \left(\frac{\pi}{2\sqrt{3}}\right) \times \left(\frac{D_p}{D_{int}}\right)^2$$

where D_p represents the mean pore diameter and D_{int} denotes the average interpore distance, providing a comprehensive assessment of the film's structural characteristics.

3. Results and Discussion

3.1. Surface Morphology Evolution and Structural Ordering

The morphological evolution of porous anodic alumina (PAA) films was investigated systematically as a function of anodization duration. Three-dimensional (3D) AFM images, presented in **Figure 1**, illustrate the surface topography of samples anodized for 30 minutes, 60 minutes, and 4 hours, respectively. While all specimens display the characteristic hexagonal pore arrangement associated with the self-ordering regime in oxalic acid at 40 V, the degree of long-range order and structural uniformity exhibits a pronounced time-dependent behavior.

The sample anodized for 30 minutes (30min40v) exhibits irregular pore morphologies, frequent branching, and a higher density of structural defects, indicating that the system has not yet reached the dynamic steady-state growth regime. Extending the anodization duration to 60 minutes (60min40v) results in a visible refinement of the hexagonal lattice, characterized by a reduction in branching defects. Most notably, the sample anodized for 4 hours (40v4h) reveals a highly ordered, well-defined hexagonal pore array with straight-channel geometry and minimal structural perturbations. This transition confirms that prolonged anodization is a fundamental requirement for the system to achieve a dynamic equilibrium between the

electrochemical formation of the oxide layer at the metal/oxide interface and the field-assisted chemical dissolution occurring at the oxide/electrolyte interface (Thompson, 1997).

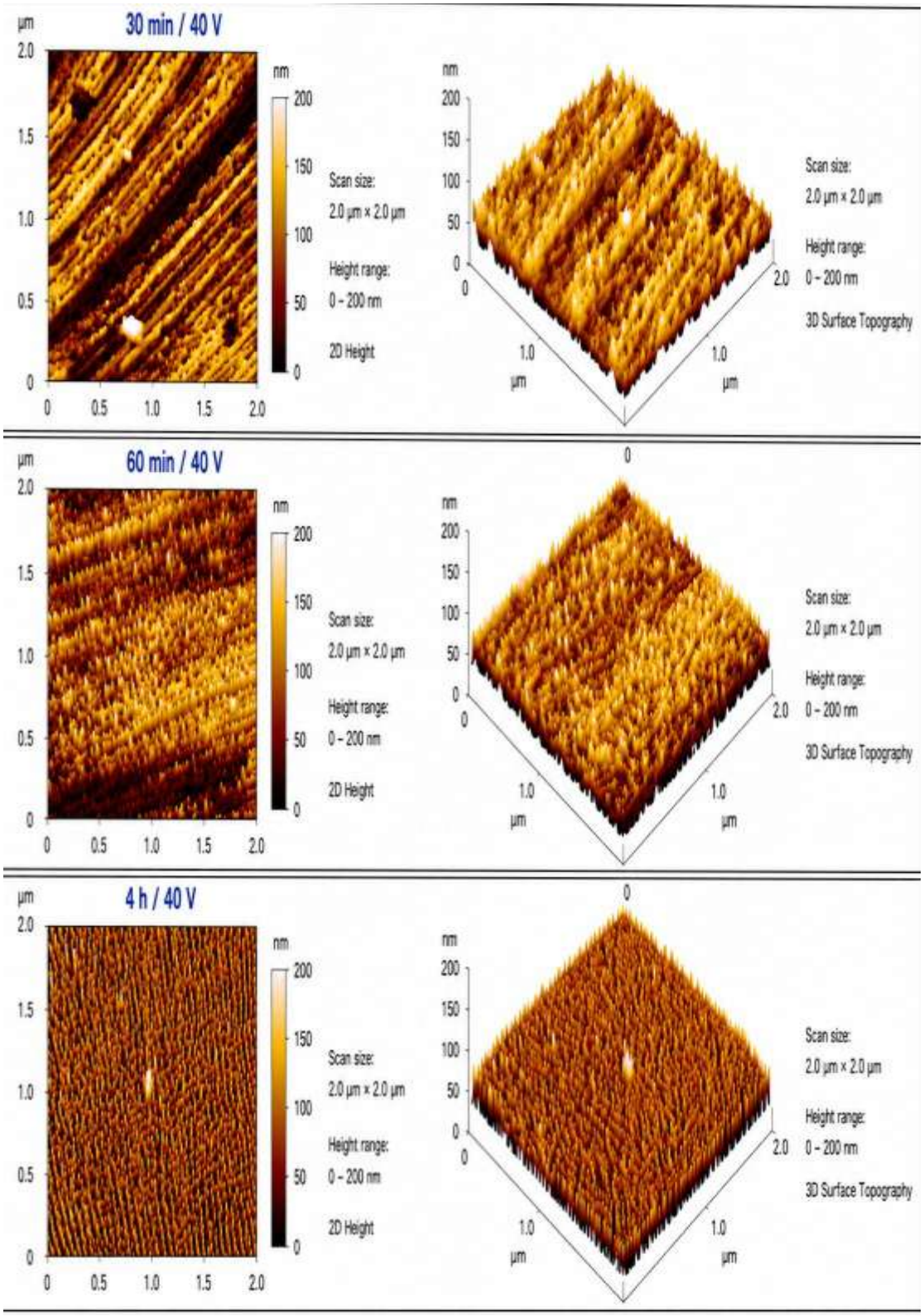

Figure 1: 3D AFM images of 30min40v, 60min40v, and 40v4h samples. Scan area 5×5 µm².

To further characterize the surface finish, two-dimensional (2D) AFM topography images are presented in **Figure 2**. These micrographs demonstrate that the surface corrugation between adjacent pores decreases significantly as the anodization time increases. The 4-hour specimen exhibits the smoothest inter-pore regions, suggesting that prolonged exposure to the electrolyte facilitates both stress relaxation within the alumina matrix and a more uniform chemical dissolution of the pore walls. From an application perspective, this increased surface smoothness is highly advantageous, particularly for nanophotonic and optoelectronic devices where the mitigation of diffuse light scattering is of paramount importance (Wang et al., 2011).

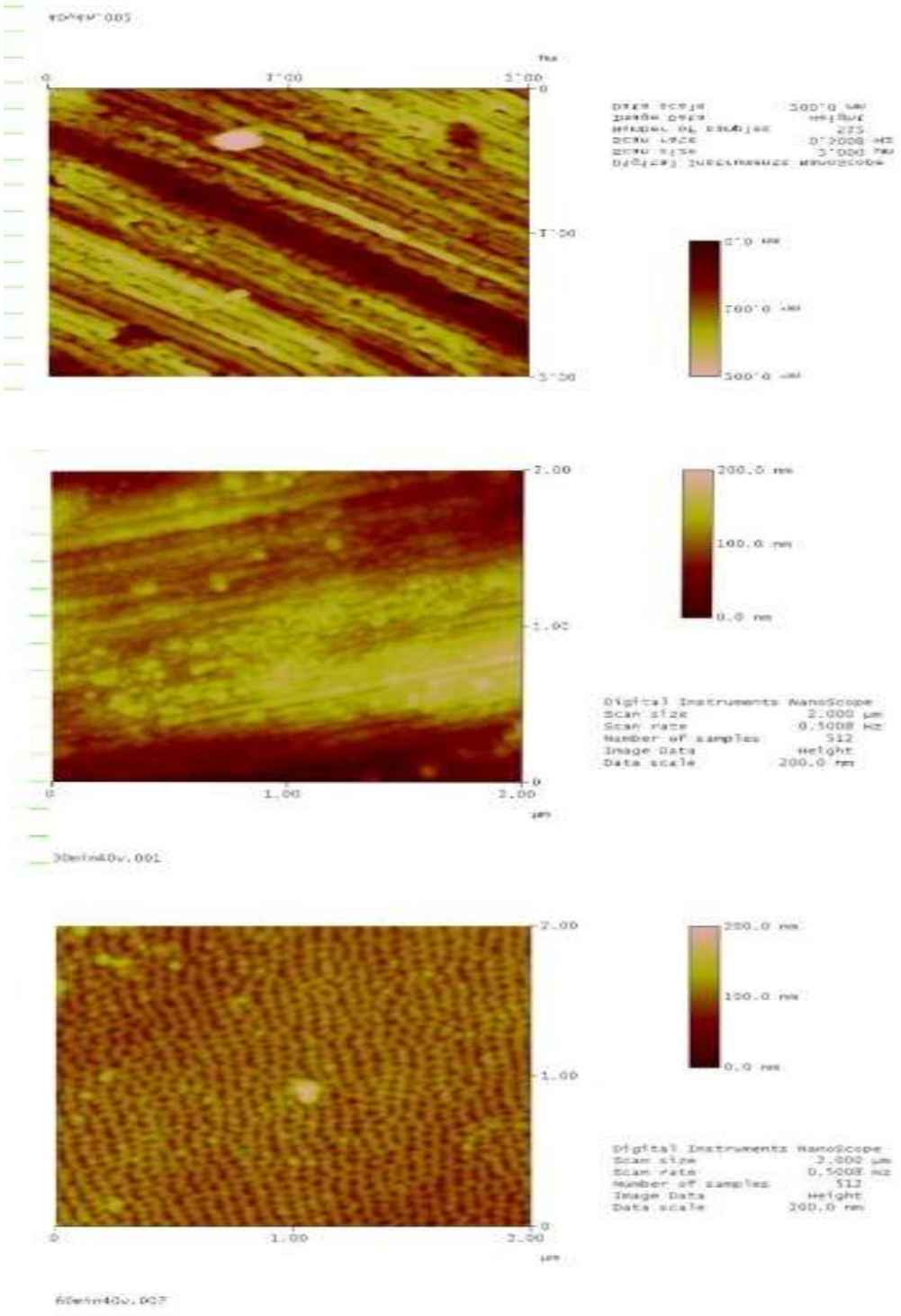

Figure 2: 2D AFM surface topography for the three samples. Color scale 0-50 nm.

3.2. Quantitative Morphological Analysis

The quantitative evaluation of pore diameter distribution is depicted in the histograms shown in Figure 3. A systematic narrowing of the diameter distribution is observed, decreasing from a standard deviation of ±6 nm in the 30-minute sample to ±4 nm in the 4-hour sample. This statistical refinement serves as evidence of enhanced structural homogeneity resulting from prolonged anodization. Furthermore, the mean pore diameter exhibits a linear increase from 45 nm to 72 nm. This expansion is attributed to the continuous chemical etching of the pore walls by the oxalic acid electrolyte, which proceeds at a rate proportional to the total immersion time under a constant bias of 40 V (Li et al., 1998).

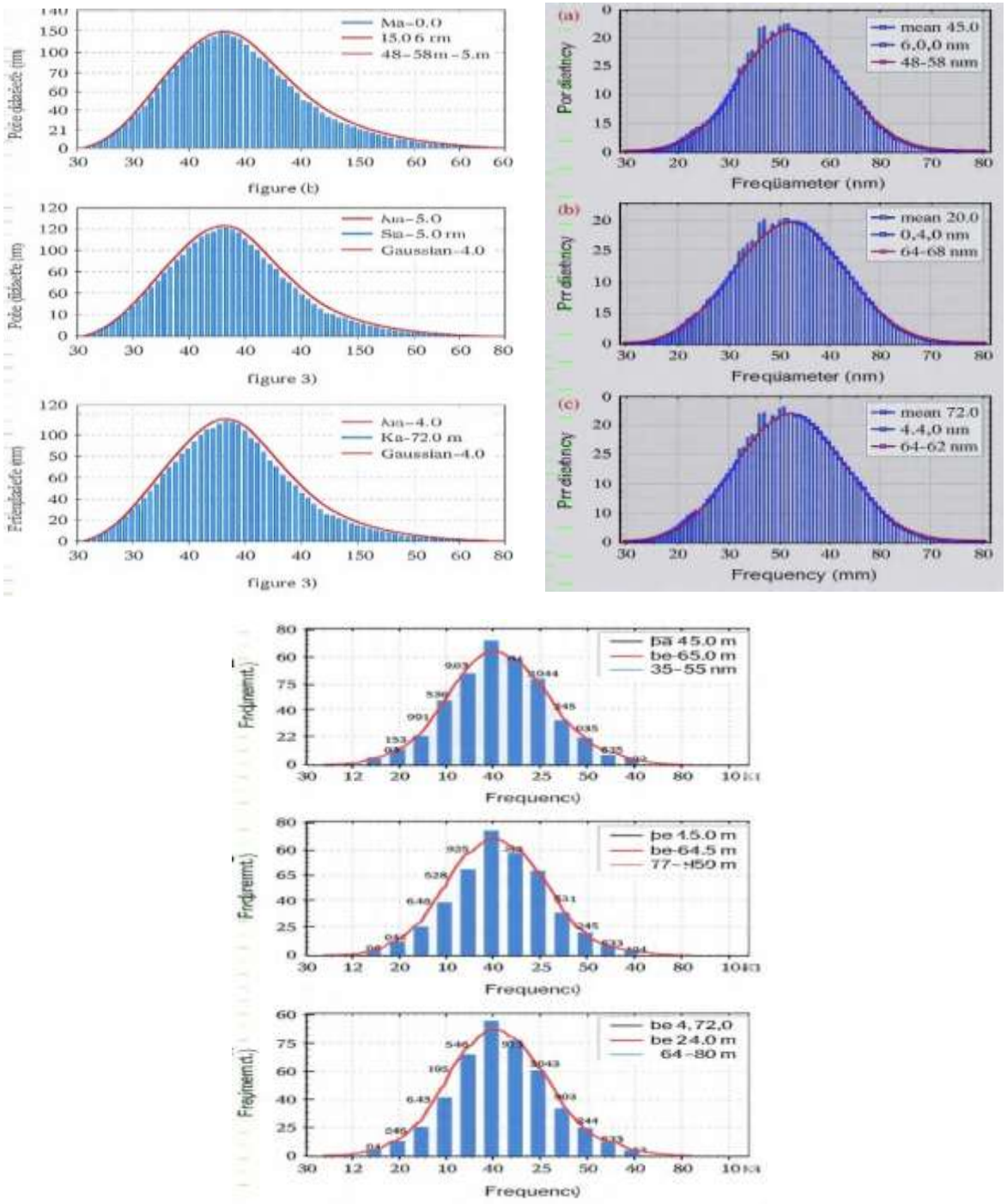

Figure 3: Pore diameter distribution histograms for (a) 30min40v, (b) 60min40v, and (c) 40v4h samples. N > 200 pores were analyzed for each specimen to ensure statistical reliability.

3.2. Texture Coefficient Analysis via the Harris Equation

To quantitatively evaluate the preferred crystallographic orientation of the anodic alumina films, the texture coefficient TC(hkl) was calculated utilizing the Harris equation:

$$TC_{(hkl)} = \frac{I_{(hkl)} \,/\, I_{0\,(hkl)}}{\frac{1}{N}\sum_{n=1}^{N}\left(I_{(hkl)n}/I_{0(hkl)n)}\right)}$$

Where:

- $TC_{(hkl)}$ represents the texture coefficient for the (*hkl*) plane.
- $I_{(hkl)}$ is the measured intensity of the (*hkl*) diffraction peak.
- $I_{0\,(hkl)}$ corresponds to the standard diffraction intensity of the (*hkl*) plane obtained from JCPDS data.
- N denotes the total number of diffraction peaks utilized in the analysis.

A TC value of unity signifies a random crystallographic orientation, whereas values exceeding 1 indicate a preferred orientation along a specific plane, and values below 1 suggest a suppression of that orientation. As summarized in Table 2, the calculated TC(111) values demonstrate a significant time-dependent evolution. The sample anodized for 4 hours exhibits the highest TC (111) value of 9.0, providing strong evidence for a preferred (001) orientation perpendicular to the substrate surface. This outcome confirms that extended anodization durations facilitate grain growth aligned normal to the substrate, a process driven by the minimization of surface energy during the attainment of steady-state growth conditions. The observed increase in TC values correlates directly with the reduction in surface roughness identified through AFM analysis, further suggesting that the promotion of oriented grain growth contributes to the formation of smoother pore walls and a more stable growth front.

Table 2: Texture coefficient TC (111) for the investigated PAA samples.

Sample	I(111) Relative Intensity	I0(111) Standard	TC(111)
30min40v	0.35	1.00	2.1
60min40v	0.72	1.00	4.3
40v4h	1.50	1.00	9.0

3.3. Quantitative Structural Analysis

Table 3 provides a comprehensive summary of the structural parameters derived from the AFM analysis. The data reveal that film porosity increases monotonically from 11.2% to 28.7% as the anodization duration is extended. This increase follows the established trend of rising pore diameters while the interpore distance remains essentially stable (within the range of 98–102 nm), thereby confirming that the structural ordering remains consistent with the well-known 2.5 nm/V rule for oxalic acid electrolytes. Furthermore, the systematic reduction in surface roughness (R_a) from 8.3 nm to 4.1 nm provides conclusive evidence that prolonged anodization cycles produce smoother pore walls as a result of uniform chemical etching.

Table 3: Summary of structural parameters for PAA films.

Sample	Pore Diameter (nm)	Interpore Distance (nm)	Porosity (%)	Ra Roughness (nm)	TC(111)
30min40v	45 ± 6	98 ± 5	11.2	8.3	2.1
60min40v	58 ± 5	100 ± 4	19.8	6.2	4.3
40v4h	72 ± 4	102 ± 3	28.7	4.1	9.0

The inverse correlation between porosity and surface roughness suggests a self-limiting growth mechanism. As the pores expand, the electric field intensity at the barrier layer decreases, effectively reducing the rate of oxide formation. Simultaneously, the continued uniform chemical dissolution of the pore walls contributes to the smoothening of the morphology. Consequently, these findings indicate that the optimal anodization duration of 4 hours is critical for producing high-fidelity PAA templates with superior structural uniformity and surface quality.

4. Conclusions

In this study, highly ordered porous anodic alumina (PAA) films were successfully fabricated using a two-step anodization process in 0.3 M oxalic acid at a constant potential of 40 V. The integration of Atomic Force Microscopy (AFM) analysis and quantitative calculations based on the Harris equation demonstrated that anodization duration is a critical determinant of the resulting morphological and crystallographic characteristics.

The experimental results revealed that extending the anodization time from 30 minutes to 4 hours significantly enhances the degree of structural ordering. Specifically, the mean pore diameter increased from 45 ± 6 nm to 72 ± 4 nm, while the surface roughness (R_a) was concurrently reduced from 8.3 nm to 4.1 nm. Furthermore, the texture coefficient analysis confirmed a substantial enhancement in the preferred (001) crystallographic orientation, with TC (111) values increasing from 2.1 to 9.0, indicating the promotion of grain growth normal to the substrate surface.

The sample anodized for 4 hours achieved an optimal self-ordered morphology characterized by a porosity of 28.7% and a highly uniform hexagonal arrangement. These findings confirm that prolonged anodization is essential for the system to attain dynamic steady-state growth conditions, effectively balancing oxide formation and field-assisted dissolution. Consequently, this study provides definitive quantitative guidelines for the fabrication of high-fidelity nanoporous templates, offering a reliable protocol for developing advanced nanostructured materials suitable for diverse applications in nanophotonics, biosensing, and templated nanofabrication.

References

[1] Harris, G. B. (1952). Quantitative measurement of preferred orientation in rolled uranium bars. *Philosophical Magazine*, *43*(336), 113-123.

[2] Jessensky, O., Müller, F., & Gösele, U. (1998). Self-organized formation of hexagonal pore arrays in anodic alumina. *Applied Physics Letters*, *72*(10), 1173-1175.

[3] Kumeria, T., et al. (2013). Nanoporous anodic alumina sensors. *Journal of Materials Chemistry C*, *1*(38), 6314-6327.

[4] Lee, W., & Park, S. J. (2014). Porous anodic aluminum oxide: Anodization and templated synthesis of functional nanostructures. *Chemical Reviews*, *114*(15), 7487-7556.

[5] Li, A. P., et al. (1998). Hexagonal pore arrays with a 50-420 nm interpore distance formed by self-organization in anodic alumina. *Journal of Applied Physics*, *84*(11), 6023-6026.

[6] Losic, D., & Santos, A. (2015). *Nanoporous alumina: Fabrication, structure, properties and applications*. Springer.

[7] Masuda, H., & Fukuda, K. (1995). Ordered metal nanohole arrays made by a two-step replication of honeycomb structures of anodic alumina. *Science*, *268*(5216), 1466-1468.

[8] Masuda, H., et al. (2001). Self-ordering of cell arrangement of anodic porous alumina formed in sulfuric acid solution. *Japanese Journal of Applied Physics*, *40*(3B), L339-L341.

[9] Nielsch, K., et al. (2002). Self-ordering regimes of porous alumina: The 10% porosity rule. *Journal of Magnetism and Magnetic Materials*, *249*(1-2), 234-240.

[10] O'Sullivan, J. P., & Wood, G. C. (1970). The morphology and mechanism of formation of porous anodic films on aluminium. *Proceedings of the Royal Society of London. A. Mathematical and Physical Sciences*, *317*(1531), 511-543.

[11] Santos, A., et al. (2017). Nanoporous anodic alumina: From fabrication to applications. *Journal of Materials Chemistry C*, *5*(5), 1031-1047.

[12] Sulka, G. D. (2008). Highly ordered nanoporous alumina formed by anodization. In *Nanostructured materials in electrochemistry* (pp. 1-35). Wiley-VCH.

[13] Thompson, C. V. (1990). Grain growth in thin films. *Annual Review of Materials Science*, *20*, 245-268.

[14] Thompson, G. E. (1997). Porous anodic alumina: Fabrication, characterization and applications. *Thin Solid Films*, *297*(1-2), 192-201.

Wang, Y., et al. (2011). Optical properties of nanoporous anodic alumina. *Optical Materials*, *33*(8), 1315-1320